Journal of Elementology ISSN 1644-2296

Svetov S., Svetova E. 2021.
Trace elements in ferruginous Marcial waters (Russia): chemical stability and mineral assays.
J. Elem., 26(2): 349-367. DOI: 10.5601/jelem.2021.26.1.2069

RECEIVED: 5 October 2020
ACCEPTED: 13 May 2021

ORIGINAL PAPER

TRACE ELEMENTS IN FERRUGINOUS MARCIAL WATERS (RUSSIA): CHEMICAL STABILITY AND MINERAL ASSAYS

Sergei Svetov, Evgeniya Svetova

Institute of Geology
Karelian Research Centre, RAS, Russia

Abstract

Marcial waters are the most famous deposit of ferruginous waters in north-western Russia. It is where Russia's oldest resort, which opened in 1719, is situated. Four water boreholes (Bh) with different water mineralization and iron content are in use today. Marcial waters have been studied for 300 years in terms of their chemical composition, mainly the content of major elements. However, precise investigations of trace elements have not been performed previously. Recently, five-year monitoring (2015-2019) of the distribution of trace elements in water boreholes and other water bodies located in the resort's area was accomplished. Also, the chemical composition (trace elements) of host rocks and the mineral phases forming them were analyzed to assess their possible contribution to the mineralization of the studied water. It has been shown that Marcial waters contain a wide range of trace elements with concentrations from 0.001 to 260 μg kg^{-1}, and displayed chemical stability for most elements during the 5 years. High concentrations of some trace elements in Marcial waters can be explained by their transfer from silicate, accessory minerals and sulfides of the host rocks. The investigations showed that waters are formed as a result of infiltration waters interacting with ore and silicate minerals, which controls the specific chemical composition. REE distribution indicates different mechanisms of their accumulation, which justifies the distinction of two contrasting water types formed as a result of mixing high-ferruginous waters of Bh 4 with infiltration water.

Keywords: ferruginous mineral water, Marcial waters, geochemistry, trace elements, REE, ICP-MS.

Evgeniya Svetova, PhD, Institute of Geology, Karelian Research Centre of the Russian Academy of Sciences (IG KRC RAS), Pushkinskaya Str. 11, Petrozavodsk, Russia, 185910, e-mail: enkotova@rambler.ru
The research was carried out within the scientific program of the IG KRC RAS.

INTRODUCTION

Ferruginous mineral waters deposits are known in many regions of the world, e.g. Marcial waters, Polustrovo, Gai, Shivanda (Russia); Neringa (Lithuania), Marianske Lazne (Czech Republic), Spa (Belgium), Roncegno Terme (Italy). The Marcial waters are the most famous deposit in north--western Russia.

The Marcial waters area is located in the Republic of Karelia (Russia), about 50 km north of Petrozavodsk (Figure 1). The first Russian resort

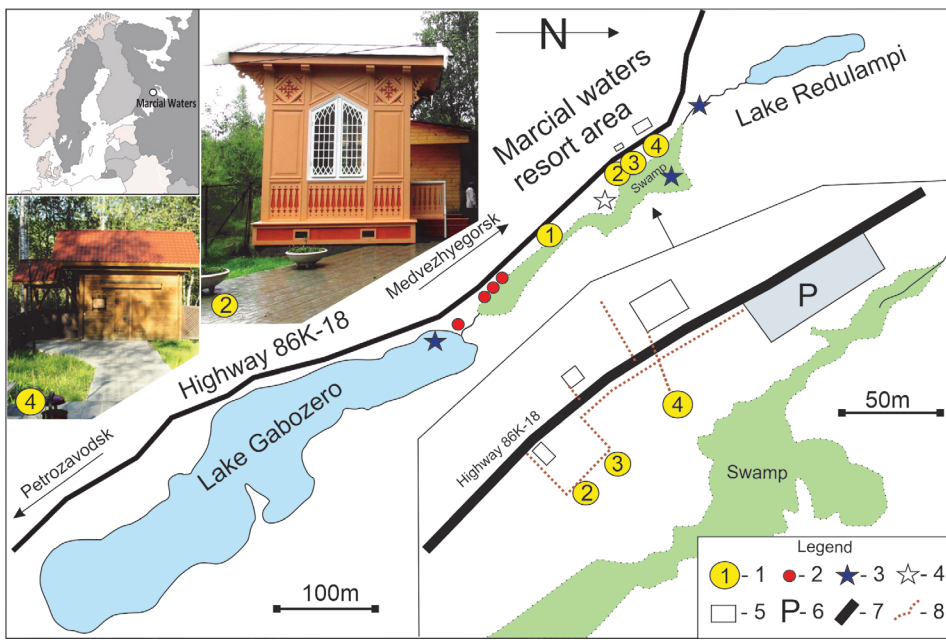

Fig. 1. Geographical location and simplified scheme of the spa resort Marcial waters: 1 – location and photos of water boreholes, 2 – unequipped Marcial waters springs, 3 – sampling site of surface waters, 4 – sampling site of snow, 5 – buildings, 6 – parking area, 7 – highway, 8 – pedestrian paths

opened here in 1719, during the reign of Peter I and with his personal participation. The resort was named «Marcial» because local waters contain a record iron (Fe^{2+}) concentration (the name refers to Mars, the god of war and iron).

Since 1964, the resort has been operating under its present status. The high-ferruginous groundwater with its unique composition is used for therapeutic and drinking purposes (helpful in treatment of anemia, blood diseases, musculoskeletal system, and nervous system). At present, the Marcial waters resort is the only resort in Karelia and among few resorts in Russia which use own mineral water, in addition to which the Marcial

waters resort uses therapeutic mud from Gabozero Lake, which has been formed with the contribution of ferruginous waters.

Four water boreholes (Bh) are operated in the resort these days (Ieshina et al. 1987, Michailov, Aminov 2006) – Figure 1. Bh 2, 3, 4 are located linearly at a distance of 20-50 m from each other, whereas Bh 1 lies 0.4 km away from them, closer to Gabozero Lake. The water of Bh 4 belongs to the high-ferruginous hydrocarbonate-sulfate type (Fe^{2+}~106 mg dm^{-3}). The other three water boreholes supply high-ferruginous waters of varying degrees contaminated by the sandy horizon waters from the Quaternary sediments. As a result, the water from these boreholes has a sulfate-hydrocarbonate composition with lower mineralization and Fe^{2+} content (mg dm^{-3}): 56 (Bh 3), 14 (Bh 1), and 41 (Bh 2). The average water characteristics are as follows: pH from 6.3 (Bh 4) to 6.0 (Bh 1-3), *Eh* (мВ) from +213 (Bh 4) to +200 (Bh 1-3), and total dissolved solids from 0.8 (Bh 4) to 0.24 (Bh 1) g dm^{-3} (Table 1).

Oxygen-free, low-acid conditions and higher CO_2 concentrations promote the formation of groundwater with high iron content. The mineral water discharge rate is 15.6 m^3/day (Michailov, Aminov 2006). The water temperature in the boreholes ranges from 4.8-5.4°C. The long-term stability of the chemical type of mineral waters with some seasonal variations in the composition are observed. Since 1990, a slight increase in sulfates and in iron concentra-

Table 1

The chemical composition of Marcial waters according to data from 1976-2012 (Tokarev et al. 2015 with appendices)

Components	Unit	Boreholes			
		Bh 1	Bh 2	Bh 3	Bh 4
pH		6.0	6.0	6.1	6.3
Eh	mV	+200	+211	+210	+213
Mineralization	g dm^{-3}	0.24	0.45	0.5	0.8
Discharge	l min^{-1}	20	40	38	6.9
CO_2	mg dm^{-3}	90	191	224	340
HCO_3^-		100	120.5	95.2	124
SO_4^{2-}		76	211	244	430
Cl^-		1.0	1.1	1.9	2.1
Na^+		3.5	4.4	4.6	5.3
K^+		2.1	4.4	4.4	5.6
Ca^{2+}		25.4	44.0	37.6	54.7
Mg^{2+}		15.2	30.0	30.6	51.0
Fe^{2+}		14	41.5	56.5	106
Fe^{3+}		<0.02	<0.02	<0.02	<0.02
Mn		0.3	0.4	0.5	0.8

tions and a decrease in the hydrocarbonate content have been observed (Tokarev et al. 2015).

The goal of this paper is to assess a possible effect of the geochemical and mineral composition of the host rocks on the mineralization of Marcial waters. The investigations included 5-year monitoring (2015-2019) of the distribution of trace elements in four water boreholes and other water bodies of the resort's territory, an analysis of the trace element composition of the host rocks and the mineral phases they are formed from, and an assessment of possible anthropogenic water pollution by high-density metals.

GEOLOGICAL SETTING

The Marcial waters area belongs to the western part of the Paleoproterozoic Onega basin (Glushanin et al. 2011). The Gabozero Lake catchment is formed from volcanogenic and volcano-sedimentary rocks of the Zaonega Formation (2.1-2.0 Ga). They are represented by massive and amygdaloidal (less often pillow) basaltic lavas, interbedded with mafic tuffs, tuffites, high-carbon and low-carbon siltstones, pellites, dolomites and siliceous tuffites (Sokolov 1972, Ieshina et al. 1987, Michailov, Aminov 2006, Glushanin et al. 2011) – Figure 2*a*.

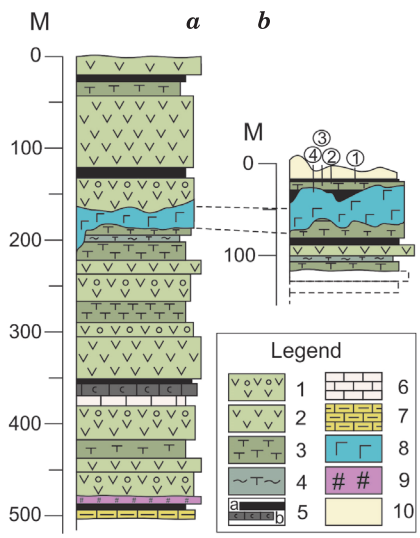

Fig. 2. Lithostratigraphic columns of Gabozero Lake (*a*) and the Marcial water resort (*b*) area (modified after Sokolov, 1972): Paleoproterozoic Zaonega Formation (1–9): 1 – amygdaloidal basalts, 2 – massive basalts (sills possible), 3 – mafic tuffs, 4 – tuffites, 5a – high-carbon siltstones, 5b – low-carbon siltstones, pellites, 6 – dolomites, 7 – siliceous tuffites, 8 – gabbrodiorite sills, 9 – peridotite sills, 10 – Quaternary rocks (soils, peats, sands, varved clays). Figure *b* shows a simplified section of the resort area (numbers in circles mark the position of the boreholes)

In the geological section, massive lavas form continual units, which are similar in both structural and mineral terms. Volcanics are represented by medium-grained and fine-grained basalts. In the medium-grained basalts, plagioclase and pyroxene crystals are replaced by chlorite, actinolite, calcite and epidote. Fine-grained basalts contain single phenocrysts of plagioclase (oligoclase-andesine) and clinopyroxene (diopside-augite) in the chlorite-actinolite matrix. Magnetite and sulfides (pyrite, chalcopyrite) are present among the accessory minerals of basalts.

Amygdaloidal and pillow basalts are characterized by medium-grained structure and diabasic texture. Plagioclase (oligoclase-andesine) and clinopyroxene (augite) are the main rock-forming minerals. Magnetite, titanomagnetite, pyrite, chalcopyrite, apatite, zircon and tourmaline are accessory minerals.

The top of lava flows is epidotized, chloritized and hematized, which reflects intense metamorphic effects and oxidation. It is important to note that basalts of effusive and subvolcanic facies are similar in mineralogical and morphological characteristics, therefore their diagnosis is difficult (some of massive lavas in the column may be sills).

Between lava units, there are lenses and beds of siliceous-carbonate and carbonate rocks. Among sedimentary rocks, there are dolomites, tuffaleurolites and tuffites of mafic composition, some of them being carbon enriched.

Intrusive rocks of the Zaonega Formation are represented by abundant bedded sills of gabbrodolerites. They are subvolcanic analogs of lavas occurring at different stratigraphic levels of the Zaonega Formation (Glushanin et al. 2011). Gabbrodolerites are similar to basalts in chemical composition but differ by the presence of gabbro textures and large tabular grains (up to 1 cm^2) of amphibolitized pyroxene, large oligoclase crystals in the altered rock, which consists of chlorite (penninite, clinochlore), actinolite, epidote, calcite and quartz. Accessory minerals are represented by apatite, tourmaline, and rare fluorite, sphalerite, titanomagnetite and magnetite. Peridotite sill (comagmatic to gabbroids) is marked at the geological section base. The age of the sill is estimated to be 1.97-1.98 Ga.

Volcanic and sedimentary rocks of the Zaonega Formation in the Marcial waters area is covered by Quaternary glacial and ice-lake sediments (total thickness up to 25-30 m). Among them, there are abundant sand and gravel deposits, loams, lenses and beds of varved clays, covered with a soil stratum on the surface (Figure 2*b*).

Water boreholes were drilled to a depth of 8-14 m down to the bedrocks. The description of geological sections of the boreholes is given from top to bottom (Ieshina et al. 1987):

– Bh 1 – loams (1.3 m), varved clays (2.2 m), sandy-rubbly sediments (1.5 m), rusty clays with pebbles and rubbles (2.9 m), argillo-arenaceous bed with basalt clasts (0.9 m), sand-gravel rocks (0.7 m – water extraction area), clays with basalt clasts (4.3 m), massive basalt lavas (0.7 m);

– Bh 2 – peat (1.5 m), loams with pebbles (0.8 m), varved clays (2.2 m), clays and loams with the lens of sand-gravel rocks (1.5 m), sands (0.75 m – water extraction area), clays with massive basalt clasts (0.75 m), massive basalts (0.5 m);
– Bh 3 – peat (1.5 m), loams (0.8 m), varved clays (2.9 m), rusty clays (0.7 m), sands with basalt clasts (0.6 m– water extraction area), rusty clays (1.3 m), basalt fault rocks (2.2 m);
– Bh 4 – peat (1 m), varved clays (2.2 m), rusty clays (1.6 m), tectonically deformed high carbon siltstones, and pellites (3.2 m), tuffites, and high carbon siltstones (2 m).

The bedrocks are tectonically deformed and cut by large fractures. It is assumed that groundwater is spatially and genetically associated with sulfidized high-carbon siltstones, mafic tuffs, tuffites on the boundary with lavas, gabbrodollerite sills and products of theirs weathering (Michailov, Aminov 2006, Tokarev et al. 2015). Water mineralization is a result of the interaction of surface waters penetrating into tectonic dislocations zones with sulfide-bearing host rocks and products of oxidation and weathering of sulfides (Ieshina et al. 1987). Sulfide phases are represented by the primary minerals of high-carbon siltstones, pellites, and the late generations of sulfides formed as a result of the thermal effect of gabbrodolerite sills on the volcanogenic--sedimentary complex. Pyrite, arsenopyrite and chalcopyrite are major sulfide minerals.

Marcial waters are fed by atmospheric precipitation and by water supplied from the Quaternary sediments. Water discharge is carried out by upward filtration through loose sediments in the Raudargiya Stream valley and Gabozero Lake basin (Tokarev et al. 2015).

MATERIALS AND METHODS

Marcial water samples from four boreholes were analyzed in June 2015, November 2016, and March 2017, 2018, 2019. Additionally, surface water samples were collected at the same time from Lake Gabozero, a small stream and a swamp and water basin (swamp) near the boreholes. These samples characterize the surface water content and reflect the process of mixing surface groundwater with Marcial waters. Snow samples were collected from the area around the boreholes to compare contents of mineral water and atmospheric precipitation.

Analytical investigations were carried out at the IG KRC RAS (Petrozavodsk, Russia). Acidified Marcial water probes (5% v/v ultrapure HNO_3) were sampled in high-density polyethylene test tubes for analysis. Trace element concentrations in water were analyzed by the ICP-MS method on an X-SERIES-2 Thermo scientific quadrupole mass spectrometer (Thermo

Fisher Scientific, Bremen, Germany). Cation analysis calibration was performed using international standards IV-STOCK-1643. Trace element contents were measured directly in the solution without pre-concentration. Analytical precision for the trace elements B, Co, Ni, Zn, Rb, Ba was <1% RSD, for Cu, As, Sr, Y, Mo, Cd, Ce, Pb was 1-5% RSD, for Li, Ti, V, Cr, Sb, La, Nd, Dy, Er was 5-10% RSD, for Zr, Nb, Pr, Sm, Eu, Gd, Tb, Ho, Er, Tm, Yb, Lu, Hf, Ta was 10-15% RSD. RSD values are derived from 10 measurements of the IV-STOCK-1643 standard prior to each analytical session.

In addition to water samples, major and trace element data of water host rock (pillow basalt sample *SV10-15* and siltstone sample *SV11-15*) were analyzed. Major elements in silicate rocks (Si, Ti, Al, Fe, Mn, Mg, Ca, Na, K, P) were determined by X-Ray Fluorescence (XRF) analyses. For XRF measurements, a powdered sample was mixed and homogenized with Li-tetraborate and analyzed using an ARL ADVANT'X-2331 spectrometer (Thermo Fisher Scientific, Ecublens, Switzerland), <5% RSD. Trace element concentrations (Li, Ti, V, Cr, Co, Ni, Cu, Zn, Rb, Sr, Y, Zr, Nb, Mo, Cd, Sb, Ba, La, Ce, Pr, Nd, Sm, Eu, Gd, Tb, Dy, Ho, Er, Tm, Yb, Lu, Hf, Ta, Pb) were determined by ICP-MS following the method (Svetov et al. 2015). Analyses were performed on 100 mg samples, which were decomposed by the acid breakdown in an open system. Samples were decomposed with high purity acids (70% $HClO_4$, 65% HNO_3, 40% HF), additionally purified by distillation in a PTFE/PFA SubboilingEcoIR acid distillatory manufactured by the High-Purity Standards Company (North Charleston, SC, USA), and deionized water. ICP-MS calibration was performed using a 68-(ICP-MS-68A-A) and 13-element (ICP-MS-68A-B) standard solutions manufactured by the High-Purity Standards Company. The SGD-2A, S-1412, and BHVO2 standard rock samples were used as certified reference samples. The study samples and reference samples were measured in groups of 15-20 with the measurements of calibration blocks to detect instrument drift in the interim. The measured concentration values are characterized by low relative standard deviation (RSD) values; the percentages are lower than 7% for most elements and 7-12%, for Cr, Zn, Co, Ni, Y, and Ta.

Trace element compositions of silicate and ore minerals were determined by LA-ICP-MS (New Wave UP 266 laser system connected to X-SERIES-2 Thermo scientific quadrupole mass-spectrometer). The LA-ICP-MS analyses were conducted on a polished rock section using a 30-70 μm beam diameter, 10 Hz frequency, and 0.13 mJ/pulse power. The instrument was calibrated against the NIST 612 standard silicate glass (National Institute Standard and Technology, Gaithersburg, USA). Calibration procedures were made at the beginning and the end of the measuring cycle and after analyzing five spots. The measured trace element concentration values are characterized following parameters of RSD: for (Cr, Co, Ni, As,) <9%, for (V, Cu, Zn, Rb, Sr, Y, Zr, Nb, Ba, Pr, Sm, Gd, Tm, Hf, Ta,) <15%, for (Ti, Li, Mo, Cd, Sb, La, Ce, Nd, Eu, Tb, Dy, Ho, Er, Yb, Lu, Pb) <20%, These values are obtained from the results of 50 measurements of the standard.

RESULTS

Most often, groundwater is not in a stable balance with original minerals, both essential (feldspar, pyroxene, hornblende, epidote, chlorite, muscovite, biotite) and accessory phases (IVANOVA et al. 2013). This leads to the active dissolution of minerals and the formation of the specific chemical composition of water as a result.

In this study, the chemical composition (trace elements) of host rocks and mineral phases forming them were analyzed to assess their possible contribution to the mineralization of the studied water.

Host rock characteristic

Basalt from Paleoproterozoic pillow lavas appears as massive fine-grained dark gray rock. The main part of the rock is composed of amphibolized clinopyroxene, albitized plagioclase, and products of change of volcanic glass. There is a significant quantity (up to 5%) of late sulfides. The top of the lava flows is highly oxidized. With respect to the chemical composition, basalts belong to the calc-alkaline type and are characterized by high MgO (up to 95 g kg^{-1}) and Fe_2O_3 (up to 140 g kg^{-1}) content (Table 2). Also, a special

Table 2

The chemical composition of Marcial water host rocks (XRF data, g kg^{-1})

Sample	SiO_2	TiO_2	Al_2O_3	Fe_2O_3	MnO	MgO	CaO	Na_2O	K_2O	P_2O_5
SV10-15 pillow basalt	502.5	16.4	118.7	140.2	2.0	91.8	89.4	35.2	1.3	2.4
SV11-15 siltstone	519.8	16.6	167.4	138.6	1.5	64.7	30.4	51.5	6.7	2.8

The chemical compositions of host rocks is given as an average of 5 samples.

feature of the rocks is the moderate concentrations of (mg kg^{-1}): Co (40-48), Ni (110-130), Cu (65-80), Zn (98-110), and high concentrations of Sr (90-280), Zr (112-140), Ba (97-170) – Table 3. Patterns of rare earth elements (REE) were normalized to Post-Archean Australian shale (PASS), (TAYLOR, MCLENNAN 1985) and the rocks were found to be depleted of light REE (LREE) – Figure 3*a*.

Paleoproterozoic siltstones are represented by fine-grained grey-brown schistose rocks with a layer thickness of about 1-3 mm. According to the composition of the petrogenic elements, siltstones differ from volcanics by higher Al_2O_3 and alkali contents, lower MgO and CaO contents. On account of the terrigenous component, siltstones are enriched with (mg kg^{-1}): Zr (200-250), Nb (20-25), Hf (4.9-5.2), Ta (1.1-1.2), and REE – Tables 2, 3, but at the same time, they have a similar spectrum topology to that of basalts of the Zaonega Formation (Figure 3*a*, Table 3).

Table 3

Trace element concentrations of host rocks (ICP-MS) and minerals (LA-ICP-MS), mg kg^{-1}

Elements	SV10-15	SV11-15	Qtz	Ab	Px	Py	Ccp	Asp	Mgt
Li	19.7	20.99	35.54	58.65	27.9	12.2	11.4	15.2	1.41
Ti	11520	13140	–	–	–	12.3	4.41	1299	718
V	285	250	225	227	119	52.2	50.4	31.5	722
Cr	278	213	57.9	46.4	347	38.6	30	24.8	463
Co	48.5	43.6	–	–	–	433	10.1	91.2	39.2
Ni	129	166	–	–	–	142	35.8	99.6	215
Cu	78.3	76.4	–	–	–	1551	46091	131	40.0
Zn	99.6	131	–	–	–	6259	138	34.9	29.6
As	–	–	–	–	–	4976	1387	138194	37299
Rb	2.54	12.8	18.9	18.6	37.4	19.64	16.97	32.1	3.03
Sr	272	96.3	195	755	368	101	23.9	116	70.2
Y	16.5	21.1	54.7	61.8	56.2	12.9	6.04	17.0	5.82
Zr	112	221	551	699	437	11.4	5.11	79.7	1.32
Nb	13.1	22.1	59.7	75.6	25.8	1.89	2.57	7.18	0.65
Mo	0.41	0.63	–	–	–	106	45.2	3.45	1.25
Cd	0.32	0.44	–	–	–	564	12.3	0.94	0.82
Sb	0.16	0.31	–	–	–	615	126	6127	0.28
Ba	97.7	166	23.4	53.5	232	2.03	1.54	99.1	4.28
La	6.79	18.5	13.7	50.2	15.4	0.61	1.23	19.3	0.24
Ce	18.9	46.3	47.3	135	17.5	2.89	1.61	22.2	0.81
Pr	2.79	5.71	7.31	14.5	9.78	0.86	0.66	2.83	0.19
Nd	14.5	25.6	25.8	61.2	35.5	1.48	4.99	9.34	0.89
Sm	3.90	5.51	9.59	19.6	9.33	0.81	1.20	1.63	0.75
Eu	1.18	1.51	1.42	1.77	2.91	0.06	0.39	0.46	0.59
Gd	4.33	5.75	4.12	5.12	10.6	0.40	0.37	2.46	0.88
Tb	0.64	0.82	0.95	2.71	2.17	0.19	0.34	0.33	0.17
Dy	3.67	4.45	13.2	17.4	8.98	1.77	0.92	2.71	1.19
Ho	0.69	0.84	1.19	3.48	2.66	0.35	0.09	0.51	0.24
Er	1.81	2.32	4.29	7.19	9.21	1.85	0.62	1.72	0.59
Tm	0.24	0.29	0.35	0.39	0.73	0.02	0.03	0.32	0.09
Yb	1.51	2.07	2.35	5.36	12.1	0.73	0.31	1.42	0.49
Lu	0.21	0.29	0.83	1.50	0.83	0.21	0.28	0.36	0.06
Hf	2.92	5.22	12.6	18.1	4.62	1.97	0.77	2.79	0.08
Ta	0.80	1.20	4.91	5.35	3.07	0.17	0.09	0.51	0.07
Pb	2.31	5.53	–	–	–	1.71	5.09	325	1.64

Explanations: SV10-15 – pillow basalt, SV11-15 – siltstone, Qtz – quartz, Ab – albitized oligoclase, Px – pyroxene (augite), Py – pyrite, Ccp – chalcopyrite, Asp– arsenopyrite, Mgt – magnetite. Trace element concentrations for all minerals are given as an average of 10 measurements; – means no data

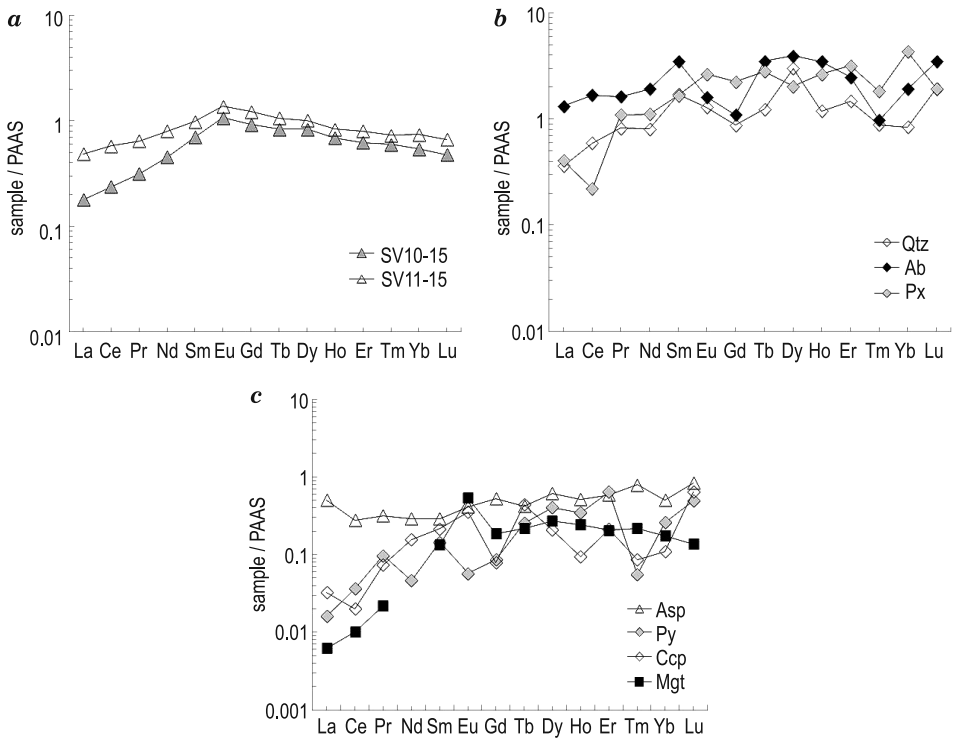

Fig. 3. REE distribution patterns (normalized to PASS (Taylor, Mclennan, 1985)) of Marcial waters host rocks (*a*), silicate (*b*) and ore (*c*) minerals of Zaonega Formation: SV10-15 – pillow basalt, SV11-15 – siltstone; Px – pyroxene (augite), Ab – albitized oligoclase, Qtz – quartz, Py – pyrite, Ccp – chalcopyrite, Asp – arsenopyrite, Mgt – magnetite

Mineral chemistry

Quartz, feldspar and pyroxene are the main silicate minerals of host rocks. Quartz contains a low level of the REE concentration. Significant concentrations of trace elements in quartz are usually associated with the presence of mineral inclusions. Pyroxene (augite) is characterized by high concentrations of V, Cr, Sr, Zr, Ba (100-450 mg kg^{-1}), Nb, Rb, Nd (20-40 mg kg^{-1}), and low concentrations of most REE (<20 mg kg^{-1}) – Table 3. Oligoclase (often substituted by albite) has high concentrations of Zr and Sr (650-800 mg kg^{-1}), Ce (130 mg kg^{-1}), Nd (60 mg kg^{-1}). REE distribution patterns of silicate minerals are depleted of LREE (Figure 3*b*).

Among ore minerals, the highest level of a REE concentration was established in arsenopyrite (next-higher order than in the other ore phases). Pyrite, chalcopyrite and magnetite are characterized by low LREE levels (Figure 3*c*). The main differences between ore phases are manifested in the content of Sb, Cd, As, Zn, Cu, Ni, V, Ti (Table 3).

Water chemistry

The chemical composition of Marcial waters has been studied for over 300 years, with a focus on major elements (Ieshina et al. 1987, Aminov 2006, Glushanin et al. 2011, Michailov, Borodulina et al. 2019). The origin of ferruginous mineral water has been described in detail (Tokarev et al. 2015). However, precise investigations of the trace element distribution in these waters have not been performed previously.

Major elements. The content of main elements in Marcial water boreholes is given according to average results from chemical composition studies carried out between 1976 and 2015 (Tokarev et al. 2015) – Table 1. Calcium predominates in the cationic composition only in the water of Bh 1 and Bh 2 (25 and 44 mg dm^{-3}). The water composition of Bh 3 and Bh 4 is dominated by iron (57 and 106 mg dm^{-3}). Concentrations of sodium and potassium in the water of all boreholes are small and amount to 2-6 mg dm^{-3}. The iron content (Fe^{2+}) increases from Bh 1 to Bh 4 (medians 14, 42, 57, 106 mg dm^{-3}, respectively). In the same sequence, the average concentration of manganese also increases from 0.3 to 0.8 mg dm^{-3}.

Trace elements. The chemical composition of studied water samples is listed in Table 4. Monitoring of the waters from Bh 1 - Bh 4 during five years (2015-2019) has revealed that water of all boreholes does not show any significant variation in the chemical composition. The spread of these values is mainly due to seasonality and the effect of atmospheric precipitation on the recharge of groundwater.

All Marcial water samples contain a wide range of trace elements, with concentrations from 0.001 to 240 μg kg^{-1}. The highest concentrations were established for (μg kg^{-1}): Zn (50-260), Ni (25-190), Co (7-40), As (30-70), Sr (33-70), Ba (3-19). Lower concentrations of (μg kg^{-1}): Li (9-13), B (18-30), Rb (2-5), Mo (1-4), Cu (0.7-19) were determined in Marcial waters. Concentrations of other elements are less than 1 μg kg^{-1}.

Studies of REE content in various types of natural water have been increasingly widespread in the last years. The main reason is the fact that REE content can be used as a marker of different geological and hydrogeological processes (Tweed et al. 2006, Möller et al. 2008, Gob et al. 2013, Chelnokov et al. 2015, Sojka et al. 2019).

ΣREE concentration in the studied water from the four boreholes is varied (Table.4). The highest REE concentration (ΣREE 0.204-0.224 μg kg^{-1}) was found in water samples from Bh 3; the lowest REE concentration (ΣREE 0.041-0.48 μg kg^{-1}) was determined in water samples from Bh 1. The water of Bh 2 and Bh 4 contains approximately equal values ΣREE: 0.134-0.141 μg kg^{-1} and 0.126-0.169 μg kg^{-1} respectively.

Normalized to PASS, all water samples are depleted of LREE and have various spectrum configurations (Figure 4). Insignificant negative cerium anomalies ($Ce/Ce^{*}=Ce_{norm}/(La_{norm}\ Pr_{norm})^{0.5}$) are present in all water samples. They range from 0.6 to 0.9. Pronounced positive europium anomalies

Table 4

Trace element concentrations of Marcial water boreholes (Bh) 1-4 (ICP-MS) analyzed in 2015-2019 (μg kg^{-1})

Elements	Bh 1					Bh 2				
Years	2015	2016	2017	2018	2019	2015	2016	2017	2018	2019
Li	9.61	8.81	8.46	8.50	8.54	12.61	10.85	10.23	10.75	11.27
B	21.41	18.37	17.7	17.85	17.99	23.13	18.88	18.65	18.87	19.10
Ti	1.32	0.61	0.66	0.84	1.02	1.40	0.66	0.89	1.01	1.12
V	1.37	0.17	0.13	0.11	0.09	1.54	0.18	0.16	0.13	0.10
Cr	0.50	0.83	0.51	0.40	0.29	0.67	0.69	0.66	0.50	0.33
Co	9.12	7.30	7.12	7.05	6.99	13.49	12.26	11.26	11.77	12.28
Ni	37.49	26.78	25.89	25.79	25.69	100.2	78.82	72.34	75.27	78.21
Cu	0.45	0.22	0.42	0.46	0.50	0.53	0.51	3.00	1.75	0.50
Zn	63.44	51.46	50.36	53.97	57.58	112.3	94.24	91.57	97.37	103.18
As	30.81	31.04	30.04	30.70	31.36	46.69	43.80	43.00	43.97	44.94
Rb	2.71	2.23	2.42	2.40	2.38	4.26	3.63	3.89	3.93	3.97
Sr	41.9	33.6	38.74	39.31	39.88	61.25	43.74	47.87	48.91	49.95
Y	0.06	0.05	0.06	0.06	0.06	0.19	0.15	0.16	0.17	0.17
Zr	0.06	0.03	0.01	0.01	0.01	0.04	0.01	0.01	0.01	0.01
Nb	0.01	0.02	0.01	0.01	0.01	0.01	0.01	0.00	0.01	0.01
Mo	3.54	2.97	2.70	2.65	2.60	2.40	2.21	2.01	2.10	2.18
Cd	0.11	0.05	0.06	0.06	0.06	0.13	0.17	0.07	0.08	0.10
Sb	0.03	0.03	0.03	0.03	0.03	0.03	0.03	0.03	0.03	0.03
Ba	13.83	12.68	14.20	16.62	19.05	8.40	8.20	8.12	10.09	12.07
La	0.002	0.005	0.004	0.004	0.004	0.002	0.005	0.005	0.004	0.004
Ce	0.005	0.008	0.006	0.005	0.004	0.010	0.011	0.011	0.009	0.007
Pr	0.001	0.001	0.001	0.001	0.001	0.002	0.002	0.003	0.002	0.002
Nd	0.007	0.009	0.009	0.007	0.006	0.024	0.023	0.021	0.020	0.019
Sm	0.003	0.003	0.003	0.002	0.002	0.012	0.012	0.012	0.012	0.011
Eu	0.003	0.002	0.003	0.002	0.002	0.007	0.005	0.005	0.005	0.005
Gd	0.005	0.005	0.006	0.006	0.007	0.027	0.027	0.025	0.024	0.024
Tb	0.001	0.001	0.001	0.001	0.001	0.004	0.003	0.004	0.003	0.003
Dy	0.005	0.006	0.006	0.005	0.005	0.023	0.022	0.021	0.021	0.021
Ho	0.001	0.001	0.001	0.001	0.001	0.005	0.004	0.005	0.005	0.005
Er	0.005	0.003	0.004	0.004	0.004	0.013	0.011	0.013	0.012	0.011
Tm	0.000	0.000	0.001	0.001	0.001	0.002	0.001	0.002	0.001	0.001
Yb	0.003	0.003	0.003	0.003	0.003	0.009	0.009	0.008	0.008	0.007
Lu	0.000	0.001	0.001	0.001	0.001	0.001	0.001	0.001	0.001	0.001
Hf	0.005	0.013	0.002	0.003	0.004	0.004	0.004	0.001	0.002	0.003
Ta	0.008	0.012	0.004	0.004	0.005	0.015	0.009	0.004	0.005	0.006
Pb	0.027	0.019	0.029	0.058	0.086	0.017	0.013	0.186	0.110	0.034
Ce/Ce*	0.76	0.82	0.73	0.60	0.46	0.90	0.69	0.69	0.66	0.62
Eu/Eu*	2.28	1.37	1.60	1.72	1.88	1.28	1.09	1.29	1.27	1.24

cont. Table 4

Elements	Bh 3					Bh 4				
Years	2015	2016	2017	2018	2019	2015	2016	2017	2018	2019
Li	12.72	12.73	11.95	12.47	13.00	9.23	11.45	10.87	11.66	12.44
B	22.79	21.89	21.18	21.19	21.19	23.73	29.31	27.56	27.44	27.32
Ti	1.44	0.77	0.88	0.98	1.08	0.80	0.53	0.24	0.50	0.75
V	1.64	0.18	0.15	0.15	0.15	1.71	0.24	0.21	0.21	0.20
Cr	0.65	0.69	0.59	0.54	0.48	0.44	0.72	0.65	0.58	0.52
Co	18.04	20.75	18.63	19.08	19.53	31.70	41.70	38.79	40.79	42.78
Ni	128.7	127.45	115.33	117.7	120.06	168.3	189.72	178.5	186.16	193.83
Cu	0.65	0.70	3.66	2.81	1.96	1.03	0.84	19.29	10.11	0.93
Zn	167.60	166.98	158.72	165.64	172.56	201.1	233.23	241.17	251.95	262.73
As	57.97	52.12	51.06	51.32	51.59	42.31	69.98	67.27	69.36	71.46
Rb	4.27	4.38	4.48	4.46	4.44	3.32	4.12	4.01	4.10	4.19
Sr	52.98	47.13	50.95	50.63	50.31	67.17	65.34	67.98	69.44	70.91
Y	0.28	0.25	0.26	0.26	0.26	0.16	0.18	0.20	0.20	0.21
Zr	0.06	0.02	<DL	0.01	0.01	0.03	0.02	0.01	0.01	0.02
Nb	0.01	0.01	<DL	0.01	0.01	0.01	0.01	<DL	0.01	0.01
Mo	2.65	2.27	2.09	2.14	2.19	0.83	1.34	1.18	1.26	1.34
Cd	0.19	0.13	0.13	0.13	0.13	0.18	0.16	0.15	0.15	0.15
Sb	0.04	0.03	0.03	0.03	0.03	0.08	0.14	0.14	0.14	0.14
Ba	7.24	8.65	7.64	9.40	11.16	3.70	5.45	4.78	6.65	8.53
La	0.002	0.007	0.004	0.004	0.005	0.003	0.007	0.005	0.005	0.005
Ce	0.013	0.016	0.013	0.011	0.010	0.015	0.018	0.018	0.016	0.015
Pr	0.004	0.004	0.003	0.003	0.003	0.003	0.004	0.005	0.004	0.004
Nd	0.037	0.036	0.033	0.032	0.032	0.032	0.044	0.041	0.043	0.044
Sm	0.024	0.020	0.019	0.018	0.018	0.012	0.016	0.016	0.015	0.015
Eu	0.010	0.008	0.008	0.008	0.008	0.005	0.005	0.006	0.005	0.005
Gd	0.045	0.046	0.042	0.040	0.039	0.022	0.034	0.033	0.033	0.032
Tb	0.006	0.006	0.006	0.006	0.006	0.003	0.003	0.004	0.004	0.003
Dy	0.037	0.035	0.035	0.033	0.032	0.014	0.018	0.019	0.019	0.019
Ho	0.008	0.007	0.008	0.007	0.007	0.003	0.004	0.004	0.004	0.004
Er	0.021	0.017	0.020	0.019	0.018	0.008	0.009	0.011	0.010	0.009
Tm	0.002	0.002	0.002	0.002	0.002	0.001	0.001	0.001	0.001	0.001
Yb	0.013	0.012	0.012	0.011	0.011	0.004	0.006	0.005	0.005	0.005
Lu	0.002	0.002	0.002	0.002	0.002	0.001	0.001	0.001	0.001	0.001
Hf	0.003	0.002	0.001	0.002	0.002	0.002	0.002	0.001	0.002	0.003
Ta	0.013	0.007	0.002	0.004	0.005	0.013	0.005	0.002	0.004	0.006
Pb	0.011	0.017	0.221	0.278	0.335	0.027	0.035	1.365	0.784	0.203
Ce/Ce*	0.65	0.67	0.70	0.62	0.54	0.90	0.71	0.69	0.66	0.63
Eu/Eu*	1.13	1.01	1.24	1.22	1.20	0.87	0.69	0.84	0.79	0.74

Trace element concentrations for all boreholes are given as an average of 6 water samples. The anomalies are defined as $Ce/Ce^*=Ce_{norm}/(La_{norm}\times Pr_{norm})^{0.5}$ and $Eu/Eu^*=Eu_{norm}/(Sm_{norm}\times Gd_{norm})^{0.5}$. < DL – below ICP-MS detection limit.

($Eu/Eu^*=Eu_{norm}/(Sm_{norm}\ Gd_{norm})^{0.5}$) occur in the water sample from Bh 1-3 (Eu/Eu*=1.01-2.28). The water of Bh 4 shows no pronounced Eu anomalies (Eu/Eu*=0.69–0.87). The occurrence of positive Eu anomaly indicates some enrichment of the solution of mineral phases europium.

For comparison, data on concentrations of trace elements in samples of surface water bodies (a stream located above the source, a swamp near the boreholes, and Goabozero Lake, to which these waters flow) and in snow from the area near the boreholes were analyzed (Figure 1, Table 5). REE patterns of Marcial waters, surface water and snow are shown in Figure 4.

Table 5

Trace element concentrations of surface water (Gabozero Lake, stream, swamp) and snow (ICP-MS, μg kg^{-1})

Elements	Gabozero Lake	Stream	Swamp	Snow
Li	1.102	9.978	12.3	0.173
B	0.004	0.004	0.134	<DL
Ti	1.15	1.35	1.24	<DL
V	0.23	0.18	0.51	0.22
Cr	0.32	0.67	0.63	0.64
Co	0.04	0.13	19.34	<DL
Ni	1.83	0.88	120.60	1.81
Cu	2.21	0.42	0.99	7.22
Zn	2.11	2.20	157.50	38.62
As	0.31	0.94	81.53	0.09
Rb	0.89	3.35	4.53	<DL
Sr	14.27	52.89	47.09	0.73
Y	0.03	<DL	0.61	32.14
Zr	0.06	0.01	0.10	0.01
Nb	0.01	0.01	0.01	0.04
Mo	0.16	0.19	3.52	0.01
Cd	0.00	0.01	0.13	<DL
Sb	0.04	0.01	0.07	<DL
Ba	3.137	25.73	10.16	6.937
La	0.024	0.002	0.062	0.014
Ce	0.045	0.002	0.151	0.015
Pr	0.006	<DL	0.021	<DL
Nd	0.035	0.002	0.174	0.009
Sm	0.006	<DL	0.072	<DL
Eu	0.002	0.002	0.021	<DL
Gd	0.005	<DL	0.133	<DL
Tb	0.001	<DL	0.015	<DL
Dy	0.005	0.001	0.103	<DL
Ho	0.001	<DL	0.018	<DL
Er	0.004	<DL	0.046	<DL
Tm	<DL	<DL	0.005	<DL

cont. Table 5

Elements	Gabozero Lake	Stream	Swamp	Snow
Yb	0.002	<DL	0.034	<DL
Lu	<DL	<DL	0.005	<DL
Hf	0.002	0.002	0.004	<DL
Ta	0.003	0.006	0.004	<DL
Pb	0.037	0.084	0.03	<DL
Ce/Ce*	0.86	0.95	0.95	
Eu/Eu*	1.29		0.83	

Trace element concentrations for all types of surface water are given as an average on 6 water samples (sampled in 2019). < DL – below ICP-MS detection limit.

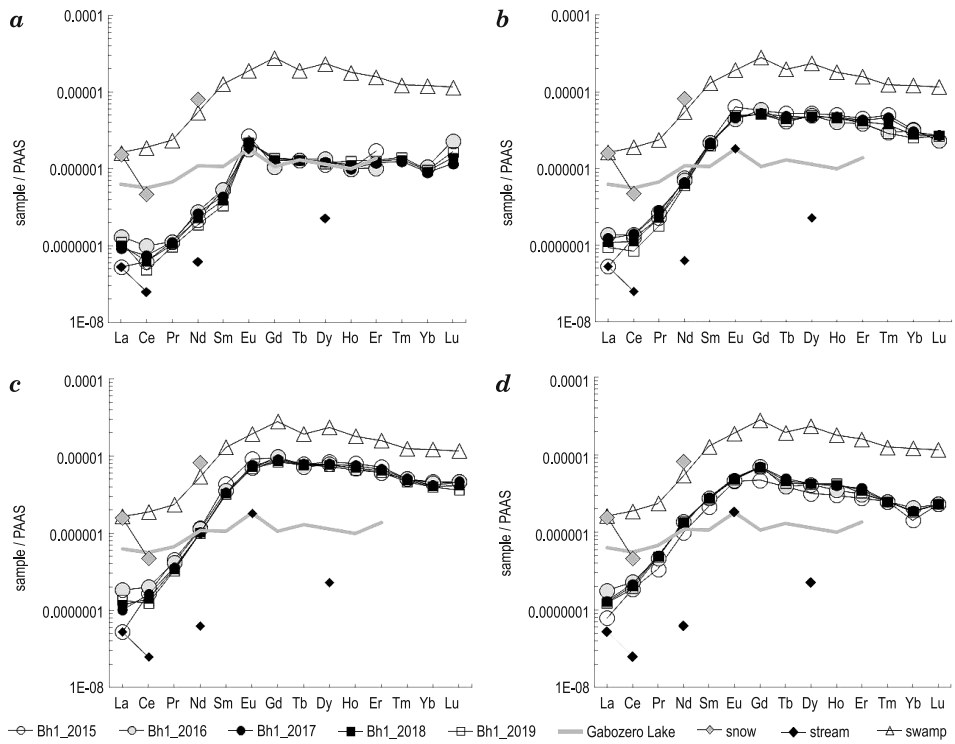

Fig. 4. REE distribution patterns (normalized to PASS (Taylor, Mclennan, 1985)) of water from boreholes (Bh 1, Bh 2, Bh 3, Bh 4) for 2015-2019, Gabozero Lake, stream, swamp, and snow (from resort area)

In snow samples, REE are contained in such low concentrations that not all of them could be determined by the ICP-MS method (Figure 4). Only La, Ce, and Nd contents were measured. It is possible that atmospheric precipitation does not make a significant contribution to the HREE and trace element content of Marcial waters, but can have some effect on their content of LREE (La, Ce, Pr, Nd). It can be assumed that the observed annual changes

in the concentration of La and Ce in the water from the boreholes may be associated with variations in the melted water volume.

The water composition of the stream flowing from Lake Redulampi (Figure 1) is characterized by extremely low REE concentrations (Figure 4). The distribution of REE in Lake Gabozero water (to which Marcial waters flow) is as close as possible to the Marcial waters in Bh 1 regarding the elements from Eu to Er. In the other boreholes, the REE level is in the next higher order. However, the content of LREE (La, Ce, Pr, Nd) is weakly depleted and the content of HREE (Tm, Yb, Lu) is below the detection limit. Thus, as water from the stream and boreholes 4-1 mixes, the content of REE in water gradually increases, forming an averaged type REE distribution in the water of Lake Gabozero.

Long-term accumulation of Marcial waters from Bh 2-4 in the swamp leads to the formation of iron hydroxide suspension (the water turns rusty), which may be the reason for the increased content of all REE in swamp water. Thus, the topology of the spectra of their distribution is preserved (Figure 4).

DISCUSSION

The process of water enrichment with iron is a result of the oxidation of sulfides in the oxygen zone and later dissolution of Fe sulfates in an oxygen-free setting. This assumption is confirmed by the mineral substitution of pyrite in high-carbon rocks with jarosite. The Fe, Mn, and Mg sulfates are characterized by high dissolubility in the temperature range of 0…–15°C and are accumulated in water during the cyclic freezing-thawing of rocks. The redox potential of the environment retains positive values all the time (Tokarev et al. 2015).

Discharged ferruginous groundwater into surface leads to iron oxidation and formation of hydroxide phases, which sorb metals from water and accumulate possible REE. This may explain the specific composition of the surface swamp waters formed by mixing Marcial waters, atmospheric water and groundwaters.

It is known that the concentration of REEs in groundwater is dependent on several factors: weathering phases, pH, redox status, adsorption, complexing ligands in groundwater and hydrogeological factors (Johannesson 2005). In the case of Marcial waters, most of these factors are identical (including the pH and redox status) except for weathering phases.

REE distribution in host rock samples is typical for Paleoproterozoic rocks of the Zaonega Formation (Glushanin et al. 2011). The level of REE content is about 3-4 times higher than in Marcial waters (Figure 4). The comparison of REE patterns of host rocks and groundwater has shown that generally water and host rocks are alike in REE distribution. The main

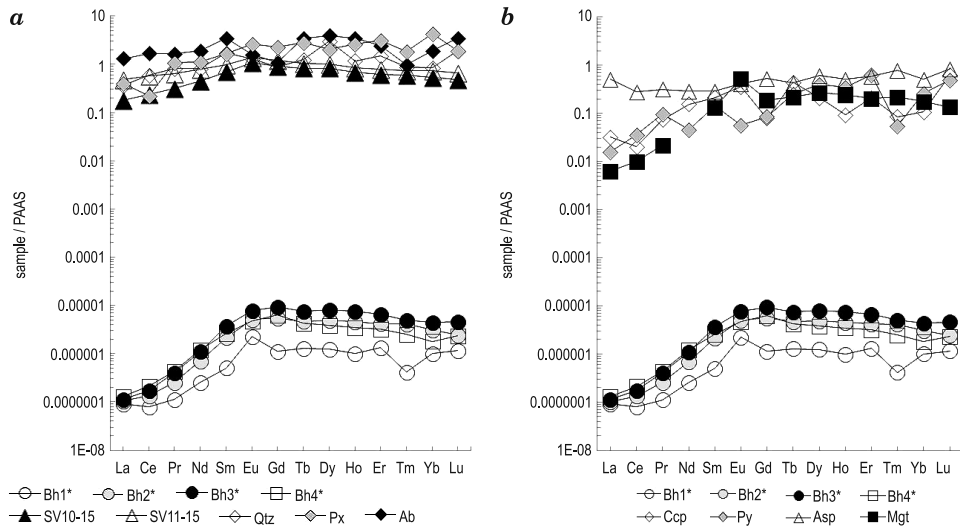

Fig. 5. REE distribution patterns (normalized to PASS (Taylor, Mclennan 1985)) of Marcial waters, host rocks, rock-forming and ore minerals of the Zaonega Formation: Bh 1 *–Bh 4 *– Marcial water boreholes (average concentrations for 2015-2019 years are given), SV11-15 – siltstone, SV10-15 – pillow basalt, Qtz – quartz, Ab – albitized oligoclase, Px – pyroxene (augite), Py – pyrite, Ccp – chalcopyrite, Asp – arsenopyrite, Mgt – magnetite.

host rock-forming minerals in the Marcial waters field are alumosilicates (pyroxene, plagioclase) and quartz. Quartz is a stable mineral in a low-temperature hydrothermal process and the REE concentration in quartz is usually lower than in pyroxene and plagioclase. Most likely, pyroxene and feldspars (plagioclase, albite, oligoclase) are supplying a significant part of REE to water. The role of the accessory phases is also important. It was previously shown that the process of pyrite oxidation is responsible for the composition of macroelements (Tokarev et al. 2015). It is important to note also that the REE distribution in pyrite, chalcopyrite and magnetite has similar, LREE depleted patterns. Furthermore, a positive Eu anomaly can be formed not only due to the destruction of plagioclase but also with the participation of chalcopyrite and magnetite (their content in basaltic lavas is about 5%). A pronounced negative Tm anomaly may also be associated with the dissolution of pyrite, chalcopyrite, albite and augite.

High concentrations of Zn, Ni, Co, As in Marcial waters can be a consequence of the interaction between water and the polymineral sulfide system (including arsenopyrite, pyrite, chalcopyrite, magnetite), while the high concentrations of Zn, Ni, and Co can be also related to the dissolution of sphalerite, millerite and cobaltite.

The Marcial water field is a tourist attraction with well-developed infrastructure: a spa resort, restaurant, museum, market and other facilities. Bh 4 is located closer than the others to the parking area (about 40 m). The analysis of the distribution of high-density metals (V, Cr, Co, Ni, Cu, Zn,

As, Cd) in water boreholes showed that the highest concentrations of these elements were in the water of Bh 4 (Table 4). A possible cause of water pollution of Bh 4 by high-density metals may be a surface water flow from the road to the borehole location area. It is known that road transport is a powerful source of environmental pollution with high-density metals. High-density metals enter the atmosphere as a part of dust with brake pad wear (Cu, Pb, Cr, Ni, Zn) and auto tyres (Zn, Cd, Cu, Pb, Al, Co, Fe, Ti), and with road pavement destruction products (Cd, Pb) (Vishnevaya, Popova 2016). This suggests the likely pollution of surface water with high-density metals, which may indirectly affect the supply reservoir.

CONCLUSION

The study of trace element distribution in Marcial waters has shown that these waters are formed as a result of infiltration waters interacting with ore and silicate minerals, which control their specific chemical composition. Despite the close pH and Eh values in all boreholes waters, the REE distribution indicates different mechanisms of their accumulation, which enables us to distinguish two contrasting water types formed as a result of mixing high-ferruginous waters of Bh 4 with infiltration water. The data on water composition during the years 2015–2019 shown the stability of water composition for REE and Zn, Mn, Ni, As, Ba and its variability for Cu, Cr, Mo, Cd, Sb. The research results indicate possible anthropogenic pollution of water by high-density metals.

ACKNOWLEDGEMENTS

We are grateful to V. L. Utitsina, M. V. Ekhova, and A. S. Paramonov (IG KRC RAS, Petrozavodsk, Russia) for their assistance in analytical investigations. We also thank Editor-in-Chief J.Elem. Slawomir Krzebietke for constructive comments, which helped us to improve the manuscript.

REFERENCES

Borodulina G.S., Tokarev I.V., Levichev M.A. 2019. *300 years of the first Russian resort. History of studies of Marcial Waters*, Problems of Balneology, Physiotherapy and Exercise Therapy, 96(4): 76-82. (in Russian) DOI: 10.17116/kurort20199604176

Chelnokov G., Kharitonova N, Bragin I, Chudaev O. 2015. *Geochemistry of mineral water and gases of the Razdolnoe Spa (Primorye, Far East of Russia).* Chelnokov et al. Appl Geochem, 59: 127-154. DOI: 10.1016/j.apgeochem.2015.05.001

Glushanin L.V., Sharov N.V., Shchiptsov V.V. (eds.) 2011. *Onega Paleoproterozoic structure (geology, tectonics, deep structure and mineralogy).* Petrozavodsk, 489 p. (in Russian)

Göb S., Loges A., Nolde N., Bau M., Jacob D.E., Markl G. 2013. *Major and trace element compositions (including REE) of mineral, thermal, mine and surface waters in SW Germany and implications for water-rock interaction,* Appl. Geochem., 33: 127-152. DOI: 10.1016/j.apgeochem.2013.02.006

Ieshina A.V., Polenov I.K., Bogachev M.A., Terukov V.S., Loginova L.F., Perskaya E.A., Borodulina G.S. 1987. *Resource and geochemistry of groundwater of Karelia*. Petrozavodsk, 151 p. (in Russian)

Ivanova I.S., Lepokurova O.E., Pokrovsky O.S., Shvartsev S.L. 2013. *Geochemistry of iron in fresh groundwater of the Sredneobskoy basin, Russia*. Procedia Earth and Planetary Science, 7: 385-388. DOI: 10.1016/j.proeps.2013.03.137

Johannesson K.H. (ed) 2005. *Rare Earth Elements in Groundwater Flow Systems*. Springer. Printed in the Netherlands. DOI: https://doi.org/10.1007/1-4020-3234-X

Michailov V.P., Aminov V.N. (ed.) 2006. *Raw mineral base of the Republic of Kareli*. Part 2. *Nonmetalic economic minerals. Undegraund waters curing muds*. Petrozavodsk, Karelia. 356 p. (in Russian)

Möller P., Rosenthal E., Dulski P., Geyer S. 2009. *Characterization of recharge areas by rare earth elements and stable isotopes of H_2O*. In: *The water of the Jordan Valley: Scarcity and Deterioration of Graundwater and its Impact on the Regional Development*. Hötzl H., Moller P, Rosental E. (Eds). Berlin Heidelberg: Springer, 123-148.

Sojka M., Siepak M., Pietrewicz K. 2019. *Concentration of rare earth elements in surface water and bottom sediments in Lake Wadąg, Poland*. J. Elem., 24(1): 125-140. DOI: 10.5601/ /jelem.2018.23.2.1648

Sokolov V.A. (ed.) 1972. *Problems of geology of the middle Proterozoic of Karelia*. Karelia, Petrozavodsk, 187 p. (in Russian)

Svetov S.A., Stepanova A.V., Chazhengina S.Y., Svetova E.N., Rybnikova Z.P., Mikhailova A.I., Paramonov A.S., Utitsyna V.L., Ekhova M.V., Kolodey B.S. 2015. *Precision geochemical (ICP-MS, LA-ICP-MS) analysis of rock and mineral composition: the method and accuracy estimation in a case study of early precambrian mafic complexes*. Writings of the Karelian researcher center RAS, 7: 54-73. (in Russian) DOI: 10.17076/geo140

Taylor S.R., Mclennan S.M. 1985. *The continental crust. its composition and evolution: an examination of the geochemical record preserved in sedimentary rocks*. Oxford; Melbourne: Blackwell Scientific Publications, 312 p.

Tokarev I.V., Borodulina G.S., Blazhennikova I.V., Avramenko I.A. 2015. *Isotope-geochemical data on ferruginous mineral waters: conditions of formation of «Marcial Waters» Resort, Karelia*. Geochem Int, 53(1): 83-86. DOI: 10.1134/S0016702914110093

Tweed S.O., Weavera T.R., Cartwrightb I., Schaeferb B. 2006. *Behavior of rare earth elements in groundwater during flow and mixing in fractured rock aquifers: An example from the Dandenong Ranges, southeast Australia*. Chem Geol, 234(3): 291-307. DOI: 10.1016/j.chemgeo.2006.05.006

Vishnevaya Yu.S., Popova L.F. 2016. *Motor transport impact on the soil cover contamination with heavy metals in the Arkhangelsk city*. Vestnik of Northern (Arctic) Federal University. Ser. Natural Sciences. 2: 32-41. (in Russian) DOI: 10.17238/issn2227-6572.2016.2.32